An Improved Marine Predators Algorithm-Based UAV Path Planning for 10-kV Distribution Networks Inspection in Live Working Scenarios

Dapeng Ma, Hongtao Jiang*, Lichao Jiang, Chi Zhang, Changwu Li, Xin Zheng, Mingxian Liu, Kai Li Yunnan Power Grid Co., Ltd., Kunming, China

Abstract—Before conducting maintenance on distribution networks, the use of unmanned aerial vehicles (UAVs) for inspecting distribution lines can effectively enhance the operational efficiency of personnel in live working scenarios. For UAV-based inspection of power distribution networks, an optimal flight path ensures both operational safety and comprehensive image acquisition in live working scenarios. Therefore, this study proposes a UAV path planning algorithm and an insulator defect classification model based on YOLOv11, aiming to develop a UAV system for live power line detection. Firstly, a UAV path planning model is established to minimize the flight path length and maximize the image acquisition range, which also considers the safety distance constraints between UAVs and live power lines. On this basis, the optimization strategy of the particle swarm optimization (PSO) algorithm is introduced into the marine predictors algorithm (MPA), and a hybrid PSO-MPA algorithm is designed to improve the convergence accuracy of the MPA algorithm and solve the proposed UAV planning model. In addition, an insulator defect detection model has been developed to accurately identify the image information collected by UAVs. In order to improve the accuracy of the YOLOv11 model, the task-separation assignment (TSA) module was introduced into the YOLOv11 model, and a TSA-YOLOv11 model was designed. Experimental results demonstrate that the proposed PSO-MPA algorithm achieves superior convergence accuracy compared to five algorithms, including PSO. When the UAV flight step size is one meter, the PSO-MPA algorithm reduces the objective function value by an average of 49.62% relative to the other algorithms. Additionally, the TSA-YOLOv11 model attained an average accuracy of 96.87% for the insulator defect classification problem.

Keywords—Marine predictors algorithm; YOLOv11; defect classification; UAV path planning; live power lines

I. Introduction

In live working scenarios, maintenance of the 10-kV distribution network by staff mainly faces challenges such as high safety risks, long inspection times, and blind spots in the field of vision. Unmanned aerial vehicles (UAVs) for inspecting 10-kV distribution networks can reduce the risk of direct exposure of personnel to high voltage environments, greatly improving safety. In addition, UAVs have multi-angle inspection capabilities, which can quickly obtain image data, significantly improving inspection efficiency and accuracy, and can timely detect hidden dangers that are difficult for humans to detect. UAV technology has the advantages of safety, high coverage, and strong defect detection capability in distribution

At present, power companies require UAVs to operate in live power line scenarios. However, the current UAV path planning problem has not taken into account the safety distance constraints between UAVs and live power lines, and there are still problems such as low convergence accuracy of path optimization algorithms [4]. In addition, the accuracy of insulator defect identification is also an important challenge. Specifically, convolutional neural network (CNN) models face challenges such as complex background interference and high training data acquisition costs in insulator defect recognition tasks. The distribution networks background of the insulator captured by UAV is too complex, such as wires, towers, sky, and vegetation, which may affect the detection accuracy of the CNN model. Therefore, it is necessary to develop an insulator defect recognition model with strong feature extraction and classification capabilities to accurately locate and identify low contrast defects on insulators in background noise. In addition, CNN models require a large amount of high-quality and accurately labeled training data during the training process. Obtaining balanced data integration that covers various defect types, camera angles, and insulator models is costly. In the context of distribution networks in reality, there are far more normal insulator samples than defect samples, which leads to CNN-based insulator defect recognition models being prone to

network inspection tasks. Therefore, the power company is exploring the application of UAVs in the inspection tasks of distribution networks. Specifically, UAV-based distribution networks inspection technology achieves accurate diagnosis of insulator defects and wire breakage faults through visual sensors [1]. In addition, UAV-based distribution networks inspection is more in line with the goals of new power system construction in terms of economy and environmental protection. For the UAV-based distribution networks inspection system, the UAV path planning module is the foundation of intelligent inspection of distribution networks. This module automatically solves an optimal and safe flight route, aiming to shorten the inspection time or distance, avoid obstacles, and ensure flight safety, ultimately achieving comprehensive image acquisition throughout the inspection range. In addition, the insulator defect detection module aims to automatically, quickly, and accurately identify various defects in insulators from a large number of inspection images, thereby effectively reducing operation and maintenance costs, preventing power grid accidents, and improving power supply reliability [2]-[3].

^{*}Corresponding author.

bias towards the "No Defects" category, significantly reducing the accuracy of defect recognition [5].

YOLOv8, as a real-time object detection model, is also used in insulator defect detection tasks. Although YOLOv8 performs better in small object detection tasks compared to

CNN models, its detection accuracy is also lower for extremely fine cracks or damages on insulators, resulting in a higher rate of missed detection of surface defects on insulators. Overall, the biggest challenges for CNN and YOLOv8 in insulator defect recognition include complex background interference and low detection accuracy for small targets [6].

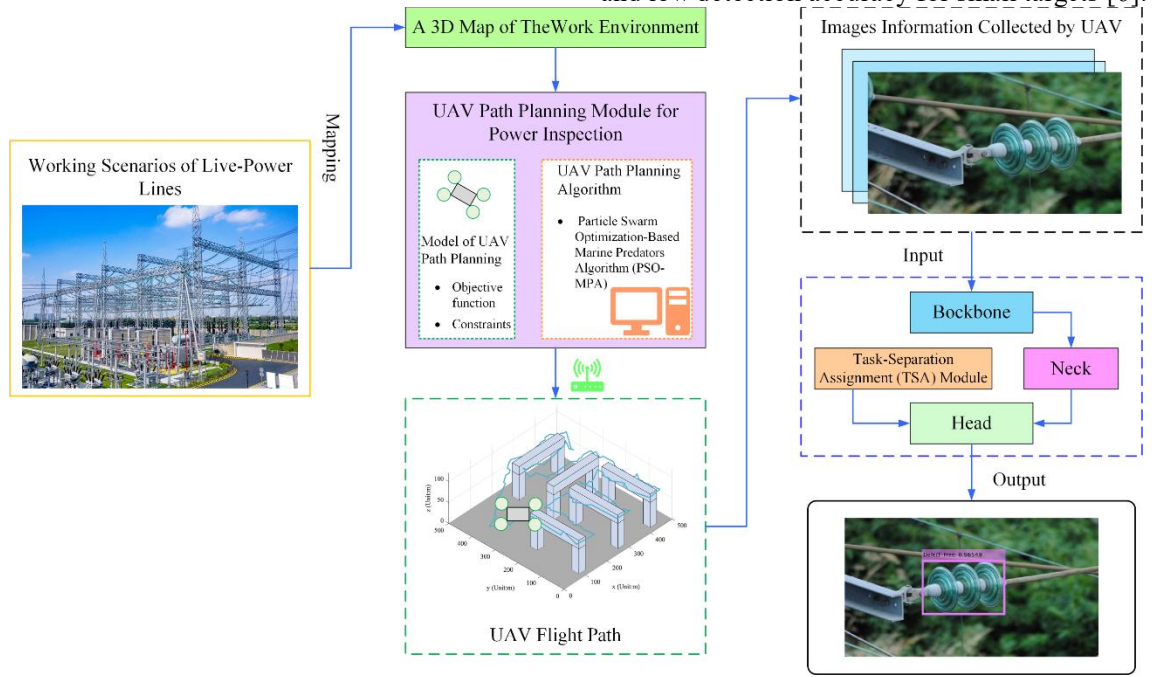


Fig. 1. UAV-based live power line inspection system.

The task paragraph assignment (TSA) module can further classify candidate samples based on specific defect types and confidence levels in insulator defect recognition tasks, thereby improving the accuracy of insulator defect recognition. Therefore, in this study, the TAS module was introduced into the head module of the YOLOv11 model with the aim of improving its accuracy. In addition, a biological heuristic algorithm has been developed to solve the optimal path for the UAV, aiming to safely and efficiently complete distribution networks detection tasks. Fig. 1 shows the UAV-based distribution networks detection system developed in this study. The system consists of two modules: UAV path planning and insulator defect recognition. The particle swarm optimizationbased marine predictors algorithm (PSO-MAP) is used to optimize the flight path of inspection UAVs. Through this flight path, UAVs can collect a large amount of image data. Based on these image data, the insulator defect recognition module identifies and detects defects in insulators. The main contributions of this study are summarized as follows:

- A UAV-based intelligent detection system framework for live power lines has been designed. The system integrates a UAV path planning algorithm and an insulator defect recognition model, and develops a complete end-to-end UAV-based distribution network detection system.
- A mathematical model for path planning for UAV power line inspection scenarios has been developed, which aims to minimize the flight path length and

- maximize the image acquisition range. In addition, the model considers the safety distance constraint between UAVs and live lines to ensure operational safety.
- A hybrid PSO-MPA algorithm was developed by combining particle swarm optimization (PSO) and marine predator algorithm (MPA) optimization strategies. Experimental results have shown that this algorithm significantly improves the convergence accuracy of the PSO algorithm, and the potential of the PSO-MPA algorithm in optimizing the path of the inspection UAV has been demonstrated.
- The TSA module was introduced into the head module of the YOLOv11 model, and the TSA-YOLOv1 model was developed to improve the accuracy of the insulator defect recognition module based on the YOLOv11 model. The TSA-YOLOv11 model achieved an average accuracy of 96.87% in insulator defect classification tasks, improving the reliability of insulator defect detection.

The remaining parts of this study are arranged as follows: Section II reviews the work on UAV path planning and defect classification. Section III introduces the proposed UAV-based distribution networks inspection system. Section IV presents the results and discusses them. Finally, Section V summarizes the entire study.

II. RELATED WORK

A. UAV Path Planning

At present, UAVs have been applied in various fields such as logistics, communication, and patrol. Therefore, a large number of UAV path planning models have been developed for these scenarios. In [7], the authors proposed an autonomous trajectory planning method for UAVs used in industrial facility inspections. This study designed a viewpoint resampling mechanism to meet the multi-perspective coverage requirements in complex industrial scenes. By dynamically optimizing the position of observation points, the image acquisition quality of key areas was improved, and the flight path length was shortened. Sonny et al. studied the path planning problem of UAV-assisted wireless networks and proposed an improved PSO algorithm [8]. In order to address the low convergence accuracy of the PSO algorithm in handling UAV path planning problems, this study introduced dynamic inertia weights and mutation operators into the PSO algorithm, aiming to enhance the algorithm's global search capability, minimize UAV energy consumption, and maximize ground user network coverage. Rückin et al. developed an active learning path planning framework for the semantic mapping of UAVs. This framework models path planning as an information gain maximization problem, evaluates the uncertainty of unexplored areas in real-time through Bayesian inference, dynamically guides UAVs to collect high-value data, and aims to plan a path for UAVs to explore unknown areas [9].

In [10], the authors propose a noise-aware path and energy management joint optimization model for collaborative operation of multiple UAVs in noise-sensitive areas. This study aims to quantify the cost of sound pollution by establishing a noise propagation model of the rotor, with the aim of constraining UAV flight altitude and path to avoid residential areas. At the same time, the study designed an intelligent power allocation strategy for batteries, aimed at maximizing the endurance of UAVs. In [11], the authors studied the challenges of UAV path planning under the framework of Internet of Drones (IoD), and proposed a distributed collaborative optimization framework. This study uses transmission delay cost and packet loss rate as path cost functions to generate paths for multiple UAVs.

In [12], the authors developed a distribution UAV autonomous path planning and control system based on the Internet of Things (IoT) and edge computing technology. The system deploys edge nodes to process UAV perception data in real-time and combines with a cloud-based task scheduling center to generate the global optimal path, significantly reducing the latency of end-to-end decision-making. The experimental results show that this path planning method can effectively reduce the communication cost and flight distance of UAVs. Yanmaz et al. developed a dynamic multi-objective path planning method to address the challenges of collaborative search and communication support for multiple UAVs. This method takes maximizing the target discovery probability and network connectivity as the objectives of the path planning model, establishes a Markov decision model, and designs a distributed UAV path optimization algorithm, aiming

to dynamically adjust the UAV formation by real-time evaluation of communication link quality [13].

In addition to the PSO-based path optimization algorithm mentioned earlier, some other cutting-edge research is also exploring the application of biological heuristic algorithms in UAV path planning problems. For example, in [14], a UAV covert path planning method based on reinforcement learning (RL) was proposed. This method is inspired by the kinematics of natural organisms, and trains RL agents to learn strategies that mimic natural organisms' covert approach to prey by constructing a three-dimensional dynamic environment of state and action space. In [15], the authors developed a UAV path planning algorithm that combines Q-learning and Grey Wolf Optimizer (GWO) to solve complex 3D path planning problems for UAV flight. This study utilizes Q-learning to dynamically optimize key parameters of the GWO, such as convergence factor and population position update weights, in order to enhance the algorithm's adaptability in dynamic obstacle environments and improve the convergence accuracy of GWO algorithm.

B. Target Identification Model

In [16], the authors designed a YOLO architecture for identifying pedestrians and vehicles for target detection tasks aimed at border patrol. In addition, this study decomposes the complex collaborative patrol problem into global path planning and local conflict resolution and task allocation problems, aiming to efficiently coordinate the flight paths and monitoring tasks of multiple drones. Chen et al. focused on the challenging problem of detecting small ship targets in ocean-wide area remote sensing images. In order to overcome the difficulties of small targets having limited information and being easily submerged in the ocean background, this study also designed an improved YOLO model, aiming to enhance the model's ability to extract features and utilize motion information of small targets, thereby improving the accuracy of ship recognition [17]. In [18], the authors developed an insulator identification and defect detection system for distribution networks inspection. This study proposes a defect detection method for insulators based on YOLOX. The core of this method lies in optimizing the YOLOX model, introducing a high-resolution differential module aimed at capturing the local detailed features and minor defects of insulators and their key components more finely.

Zhang et al. proposed a method for identifying the working angle of a loader bucket based on the YOLOv5s model. This method utilizes YOLOv5s to quickly and accurately locate the target of the bucket, and introduces an attention mechanism to more accurately recognize the posture of the bucket, ultimately calculating the working angle of the bucket [19]. In [20], the authors focus on the task of detecting small targets in infrared images. In order to solve the problem of target loss or false alarm caused by traditional methods, this study proposes an improved strategy based on pixel extension. In [21], the authors developed an intelligent inspection system based on a UAV for power insulator inspection tasks under complex weather conditions. The system has successfully achieved autonomous positioning, state recognition, and defect detection of insulators by equipping sensors and machine learning algorithms suitable for complex environments. Xuan et al.

proposed an intelligent identification method for insulator defects based on Fully Convolutional One Stage (FCOS). The experimental results show that this method can not only accurately locate and segment individual insulators in the image, but also finely segment the defect areas on the insulator surface [22]. In [23], the authors proposed an efficient personal protective equipment detection model based on YOLOv8, aiming to develop a system for detecting whether workers are wearing compliant personal protective equipment, such as safety helmets, reflective clothing, and gloves, and to improve the accuracy and robustness of the YOLOv8 model in human protective equipment detection tasks.

III. METHODOLOGY

As shown in Fig. 1, the proposed UAV-based distribution networks inspection system consists of two parts: path planning and insulator detection. The UAV path planning model aims to minimize the flight path length and maximize the image acquisition range, while considering three constraints: the maximum pitch angle, maximum endurance time, and safe distance between the UAV and the live-line. On this basis, a PSO-MPA algorithm was developed for the path planning model of power inspection drones to solve the flight path of the drones. The TSA module was introduced into the YOLOv11 model to improve the accuracy of the insulator defect recognition model.

A. UAV Path Planning for Power Inspection

Before conducting UAV path planning, the transmission facilities are first divided into grids. In this study, the transmission facilities were surface divided into a set $V = \{v_1, v_2, v_{b_{\max}}\}$. Based on the height of the transmission facilities, the initial flight height of the drone was determined as H_{fly} . The UAV's path consists of a series of path nodes $\Gamma = \{1, 2, \dots, m\}$. Another key parameter for UAV path planning is $Step_Size$.

The path distance cost $f_{Path\ Dis}$ of UAV is defined in Eq. (1):

$$f_{Path_Dis} = \sum_{m \in \Gamma} \sqrt{(x_m - x_{m-1})^2 + (y_m - y_{m-1})^2 + (z_m - z_{m-1})^2}$$
(1)

where, (x_m, y_m, z_m) is the position of the UAV's path node m in the coordinate system.

The definition of *Step_Size* is as follows in Eq. (2):

Step_Size =
$$\sqrt{(x_m - x_{m-1})^2 + (y_m - y_{m-1})^2 + (z_m - z_{m-1})^2}$$

 z_m is defined in Eq. (3):

$$z_m = H_{flv}, \forall m \in \Gamma \tag{3}$$

The image acquisition range of the UAV is defined as Eq. (4):

$$f_{img} = \frac{\sum \beta(v_b)}{b_{\text{max}}}, \forall b \in \{1, 2, \dots, b_{\text{max}}\}$$
 (4)

where, $\beta(v_b)$ is a 0-1 variable. When the UAV captures an image of grid v_b position, $\beta(v_b) = 0$; Otherwise, $\beta(v_b) = 1$.

The objective function of the UAV path planning model used for distribution networks inspection is Eq. (5):

$$F = w_1 \times f_{Path Dis} + w_2 \times f_{img} \tag{5}$$

where, w_1 and w_2 are the weight coefficients of the objective function.

The constraint conditions for UAV path planning in distribution networks inspection are defined as follows [Eq. (6)]:

$$\theta_{m} \le \theta_{\max}, \forall m \in \Gamma$$
 (6)

where, θ_m is the pitch angle of the distribution networks inspection UAV. θ_{max} is the maximum pitch angle of the distribution networks inspection UAV [Eq. (7)].

$$\frac{f_{Path_Dis}}{speed_{UAV}} \le T_{UAV} \tag{7}$$

where, $speed_{UAV}$ is the flight speed of the distribution networks inspection UAV. T_{UAV} is the maximum endurance time of the distribution networks inspection UAV [Eq. (8)].

$$L(v_b, UAV) \ge L_{safety}, \forall b \in \{1, 2, \dots, b_\max\}$$
(8)

where, $L(v_b, UAV)$ is the distance between the UAV and the distribution networks. L_{safety} is the safe distance between the UAV and the distribution networks.

To solve this path planning model, a PSO-MPA algorithm was developed. The MPA algorithm mainly includes predation strategies based on Brownian motion and target aggregation strategies based on Levy motion [24]. In order to improve the convergence accuracy of MPA, a speed update-based foraging strategy based on the PSO algorithm is also added to the hybrid PSO-MPA algorithm. The definition of the PSO-MPA algorithm is as follows:

- 1) Initialization: Initialize the position O of the marine predator population, initialize the speed of PSO, and set the maximum iteration number *Iter*_max of the PSO-MPA algorithm.
- 2) Calculate adaptive parameters: Determine the update and search process that should be executed for the current iteration count *Iter* based on the value of *Iter | Iter_* max.
- 3) Update strategy 1: The foraging strategy based on speed updates the positions of all marine predators to obtain O^{Δ} .
- 4) Update strategy 2: Based on Brownian motion, update the positions of some marine predators using a predation strategy. The update process is defined as Eq. (9):

$$O(k) _new = PBM(O(k)^{\Delta})$$
(9)

where, O(k) is defined as the location of the k-th marine predator. PBM(.) is defined as a predation strategy based on Brownian motion.

- 5) Update strategy 3: Implement a target aggregation strategy based on Levy motion for the remaining marine predators.
- 6) Evaluate and select the optimal solution: Calculate the fitness of all updated positions of marine predators and generate the optimal solution.

B. Defect Detection of Insulators

Although multiple frameworks such as Real-Time Detection Transformer (RTDRTR), Region-based Convolutional Neural Networks (RCNN), and YOLOv8 have been used for specific object detection or insulator defect identification tasks, improving the accuracy of insulator defect detection models remains a challenge [23]. Therefore, in this study, the TSA module was introduced into the YOLOv11 model to improve the accuracy of insulator defect detection. Fig. 2 shows the header module of the proposed TSA-YOLOv11 model.

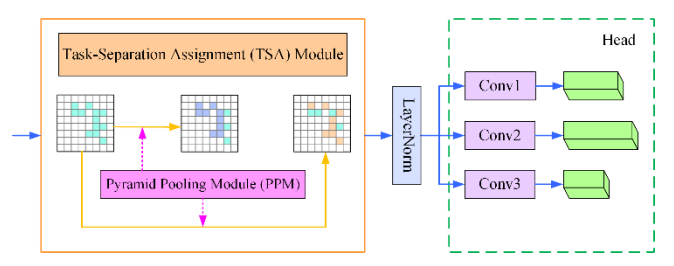


Fig. 2. Head module of the YOLOv11 model based on TSA (TSA-YOLOv11).

The header module of the TSA-YOLOv11 model is designed to enhance the recognition of insulator defect types by integrating the global modeling capability of the Transformer with the local feature extraction ability of CNN. After a series of convolutional layers and Bottleneck modules for dimensionality reduction and local feature extraction, the resulting insulator features are fed into the TSA module. Within this module, the features undergo multi-head integration, residual connections, and layer normalization before being output, thereby modeling dependency relationships between any two spatial positions.

In the header module of the TSA-YOLOv11 model, the pooling layer uses max pooling technology. The definition of max pooling is as follows [Eq. (10)]:

$$\begin{aligned} \mathbf{H}_{j} &= Rand(0,1) \times \max \left\{ \mathbf{A}_{i}, i \in P_{j} \right\} \\ &+ (1 - Rand(0,1)) \times \frac{1}{\left| P_{j} \right|} \times \sum_{i \in P_{j}} \mathbf{A}_{i} \end{aligned} \tag{10}$$

where, Rand(0,1) is a random number with a value of 0 or 1. H_j is the j-th element of the feature map output from the max pooling operation. A_i is the i-th position of the j-th element in the input feature map P_i .

IV. EXPERIMENTS

This study proposes an intelligent UAV inspection system for distribution networks detection, with a primary focus on addressing UAV path planning and insulator defect detection challenges. To validate the effectiveness of the proposed path planning algorithm, a three-dimensional flight simulation environment was established based on actual substation map data. For insulator defect detection, the image samples were collected under varying lighting conditions, shooting distances, and camera angles to ensure comprehensive coverage of operational scenarios.

A. Path Planning Results

In order to demonstrate the application results of the proposed PSO-MPA algorithm in the path planning problem of power inspection UAVs, and to explore the influence of the key parameter of flight step size on the objective function, multiple power inspection UAV path planning experiments were designed based on different flight step sizes. Firstly, the flight step sizes were set to 1 meter, 3 meters, 5 meters, 7 meters, 9 meters, and 11 meters, respectively. Based on different flight step sizes, independent experiments were conducted to explore the influence of flight step sizes on the fitness function. In addition, rime (RIME) optimization algorithm [25], Harris hawks optimization (HHO) [26], snow geese algorithm (SGA) [27], PSO, The Tornado optimizer with Coriolis force (TOC) algorithm is also used to solve the path planning problem of power inspection UAVs, aiming to verify the convergence accuracy and robustness of the PSO-MPA algorithm. In addition, in this study, standard deviation was used to evaluate the stability of the path planning algorithm for power inspection UAVs.

Fig. 3 shows the flight paths generated by the PSO-MPA algorithm for the power inspection UAV under different step sizes. Fig. 4(a) and Fig. 4(b) show the iterative function curves of PSO-MPA, HHO, PSO, RIME, SGA, and TOC algorithms with step sizes set to 1 meter and 3 meters, respectively. Fig. 5(a) and Fig. 5(b) show the iteration function curves of each algorithm when the step size is set to 5 meters and 7 meters, respectively. Fig. 6(a) and Fig. 6(b) show the iteration function curves of each algorithm when the step size is set to 9 meters and 11 meters, respectively. Table I shows the fitness function values of each algorithm at different step sizes.

From Fig. 4(a), it can be seen that the PSO-MPA algorithm generates a fitness function value of 3175.06 in solving the path planning problem of the power inspection UAV. Compared with the other five algorithms, the PSO-MPA algorithm has the smallest fitness function value, when the flight step size of the UAV is 1 meter. From Fig. 4(b), it can be seen that when the UAV's flight step size is 3 meters, the PSO-MPA algorithm also has the lowest fitness function value, which is 3276.60, an average decrease of 44.53% compared to the other five algorithms. From Fig. 5(a) and Fig. 5(b), it can be seen that when the UAV's flight step size is 5 meters and 7 meters, respectively, compared with HHO, PSO, RIME, SGA, and TOC algorithms, the fitness function value of PSO-MPA algorithm is also the smallest. From Fig. 6(a) and Fig. 6(b), it can be seen that when the UAV's flight step size is 9 meters



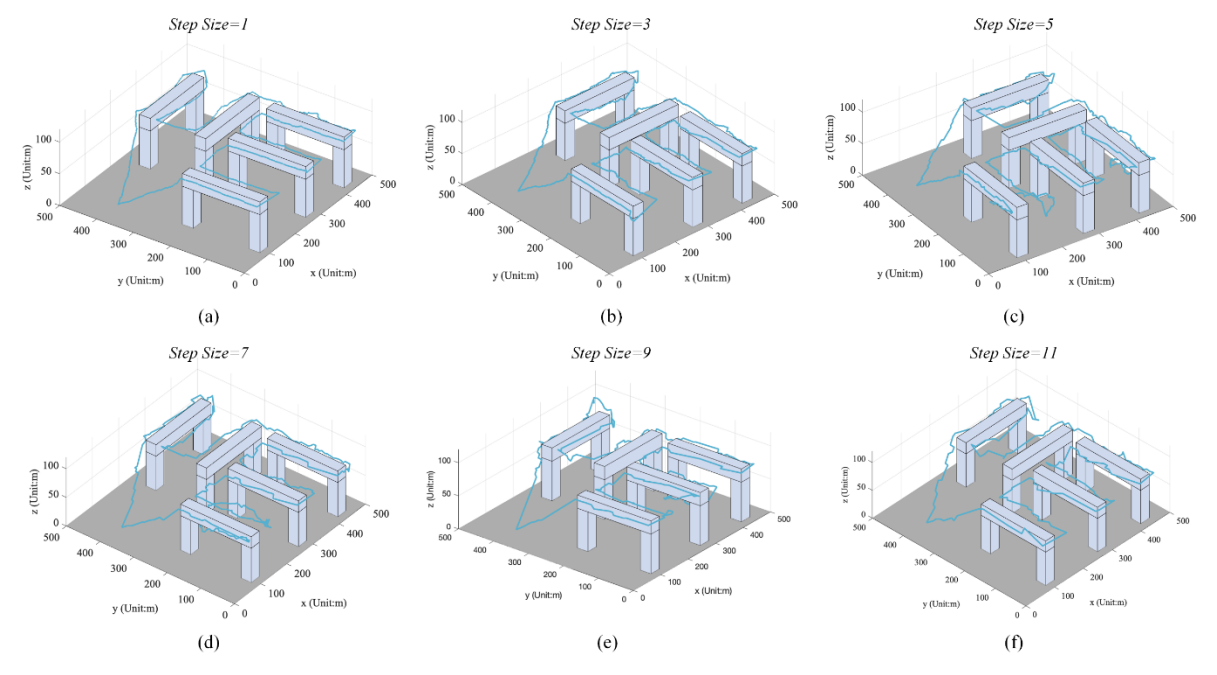


Fig. 3. UAV path planning results with different flight step sizes.

TABLE I. THE FITNESS FUNCTION VALUES OF UAV PATHS WITH DIFFERENT FLIGHT STEP SIZES

Algorithm	PSO-MPA	ННО	PSO	RIME	SGA	TOC
Step Size	Fitness Function					
1	3175.06	6665.64	6328.04	7242.72	8539.11	4343.94
3	3276.60	7626.56	6115.06	5133.10	7717.98	4396.74
5	3790.45	10572.84	7185.90	5184.23	7727.14	5169.95
7	3909.39	7121.22	6995.10	7638.17	7819.61	7842.44
9	3559.49	7914.00	7252.17	6775.45	8759.74	7146.64
11	3232.06	7058.16	5329.62	6135.50	5515.12	5837.17

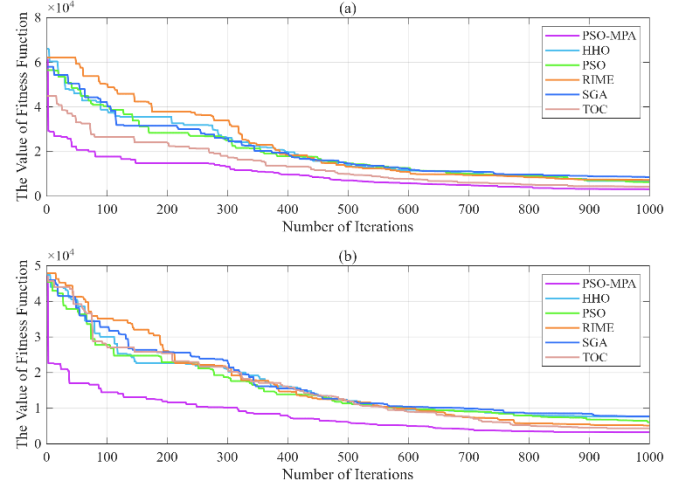


Fig. 4. The iterative function curve for flight steps of 1 meter and 3 meters.

Therefore, it can be concluded that among all step settings, the proposed PSO-MPA algorithm generates the smallest fitness function value compared to other algorithms when solving the path planning problem of power inspection UAV. The PSO-MPA algorithm performs significantly better than HHO, PSO, RIME, SGA, and TOC algorithms in solving path planning problems for power inspection UAVs. The objective function value corresponding to the PSO-MPA algorithm decreased by 25.48% to 47.46% compared to the objective function value generated by the suboptimal algorithm. When the step size is set to 9 meters, the fitness function value of the PSO-MPA algorithm is 3559.49, and the decrease in the objective function value is the most significant. Compared with the second ranked RIME algorithm, the objective function value of the PSO-MPA algorithm has decreased by 47.46%.

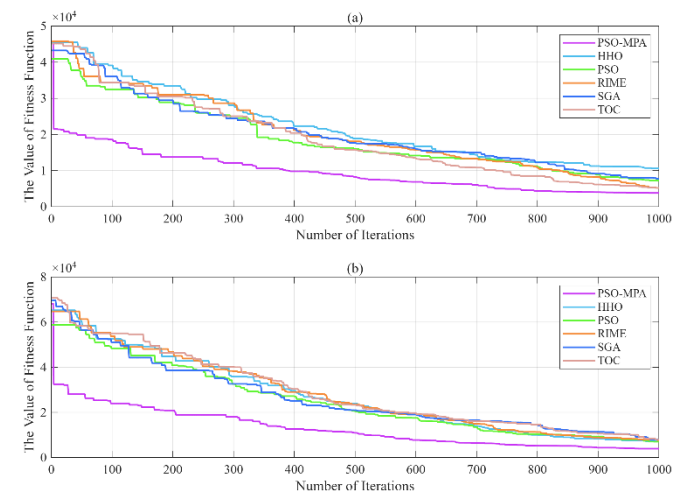


Fig. 5. The iterative function curve for flight steps of 5 meters and 7 meters.

When the step size is set to 3 meters, the performance of the PSO-MPA algorithm decreases, but compared with HHO, PSO, RIME, SGA, and TOC algorithms, the PSO-MPA algorithm still maintains a significant advantage in solving the path planning problem of power inspection UAVs. Compared with the second ranked TOC algorithm, the fitness function value of the PSO-MPA algorithm is reduced by 25.48%. In addition, by comparing the fitness values of each step size setting corresponding to the PSO-MPA algorithm, a flight step size of 1 meter was determined to be the optimal setting, and the generated drone path cost was the lowest.

Table II shows the standard deviation of the fitness function values generated by each algorithm running independently ten times at different step sizes. Fig. 7 shows the standard deviation of the objective function values generated by running different algorithms ten times with different step sizes. It can be seen that compared with HHO, PSO, RIME, SGA, and TOC algorithms, PSO-MPA is the overall most stable algorithm. The PSO-MPA algorithm achieved the minimum standard deviation in all five step settings, indicating that it can maintain high consistency under different parameters. Especially when step size is 5 meters, the standard deviation of the PSO-MPA

algorithm reaches 95.93, indicating the highest stability. HHO is the most unstable algorithm overall, with a standard deviation exceeding 270 under multiple flight step settings, significantly higher than other algorithms.

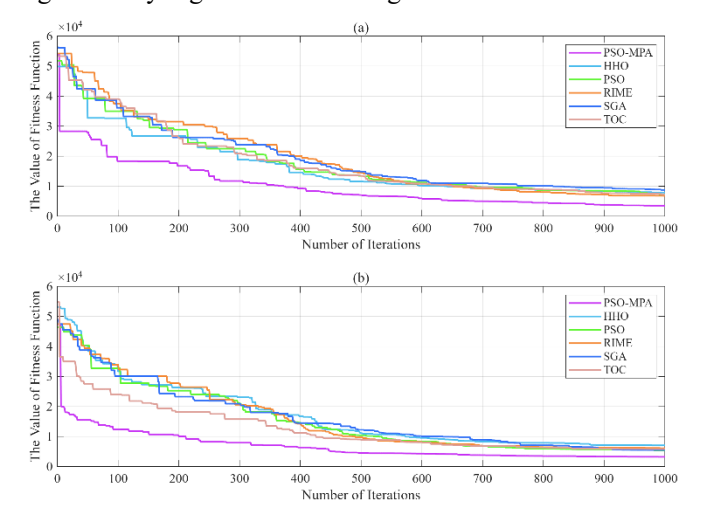


Fig. 6. The iterative function curve for flight steps of 9 meters and 11 meters.

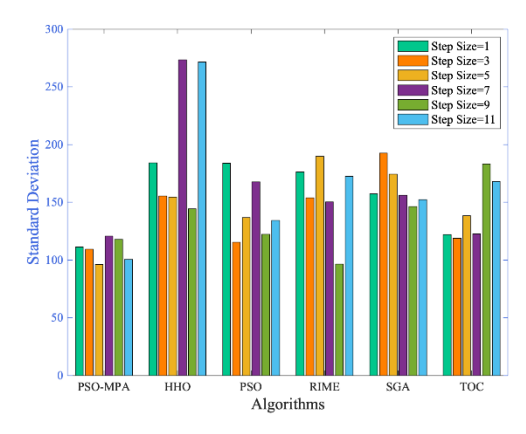


Fig. 7. The standard deviation of the fitness function values for UAV paths with different flight step sizes.

TABLE II. THE STANDARD DEVIATION OF THE FITNESS FUNCTION VALUES FOR UAV PATHS WITH DIFFERENT FLIGHT STEP SIZES

Step Size	Step Size=1	Step Size=3	Step Size=5	Step Size=7	Step Size=9	Step Size=11
Algorithm	Standard Deviation					
PSO-MPA	111.25	109.27	95.93	120.58	117.73	100.46
ННО	184.11	155.46	154.54	273.41	144.24	271.39
PSO	183.61	115.22	136.78	167.78	122.32	134.26
RIME	176.18	153.63	189.80	150.17	96.32	172.27
SGA	157.26	192.48	174.19	156.14	146.22	152.15
TOC	121.82	118.70	138.26	122.44	183.05	167.97

B. Defect Detection Results of Insulators

To verify the performance of the TAS-YOLOv11 model in insulator defect detection, insulator defect detection experiments were conducted based on the RTDETR model, R-CNN model, YOLOv8 model, YOLOv10 model, and

YOLOv11 model [28]-[30]. Table III shows the types of insulator defects included in the training and testing sets of this study. In this study, insulators used in distribution networks were classified into four types: defect free, defect type 1, defect type 2, and defect type 3.

In this study, the dataset includes 8000 insulator images. The number of images in each of the four categories (insulators without defects, defect type 1, defect type 2, and defect type 3) is 2000. The training set includes 1600 insulator images for each of the four categories. The test set includes 1000 insulator images for each of the four categories. Table IV shows the parameter settings for different models. For different insulator defect detection models, the batch size and number of epochs are 2 and 300, respectively.

TABLE III. DEFECT TYPES OF INSULATORS

Class	Definition			
Defect-Free	No defects: The insulator has no defects and works normally.			
Defect Type 1	Surface Defect: The material on the surface of the insulator is damaged.			
Defect Type 2	Damaged: The edge of the insulator is damaged or there are cracks in the insulator.			
Defect Type 3	ect Type 3 Missing: The insulator string is missing one or severa insulators.			

Table V presents the mean average precision (mAP@0.5) and training loss values for different insulator defect detection models. The proposed TAS-YOLOv11 achieves an mAP@0.5 of 95.16%, outperforming the RTDETR and R-CNN models by 11.08% and 6.43%, respectively. Additionally, its training loss is 0.1252, representing reductions of 37.59% and 36.28% compared to RTDETR and R-CNN, respectively. Compared with the RTDETR model, R-CNN model, YOLOv6 model, YOLOv8 model, YOLOv10 model, and YOLOv11 model, the mAP@0.5 index of TAS-YOLOv11 increased by an average of 5.14%, and the training loss of TAS-YOLOv11 decreased by an average of 28.49%. Fig. 8 shows the results of insulator defect recognition based on the TAS-YOLOv11 model.

TABLE IV. PARAMETER SETTINGS

Models	Parameter	Value	
	Batch size	2	
RTDETR	Number of epochs	300	
	Learning rate	1E-4	
	Batch size	2	
R-CNN	Number of epochs	300	
	Learning rate	1E-6	
	Batch size	2	
YOLO	Number of epochs	300	
	Learning rate	1E-3	

Table VI shows the performance of different insulator defect detection models. In Table VI, two indicators, accuracy and recall, are used to evaluate different insulator defect detection models. From Table VI, it can be seen that in the experiment of insulator defect detection, the TAS-YOLOv11 model has the best performance and highest accuracy in the four types of defect detection.

TABLE V. PERFORMANCE COMPARISON OF DIFFERENT MODELS

Models	mAP@0.5 (%)	Training Loss
RTDETR	85.67	0.2006
R-CNN	89.41	0.1965
YOLOv8	91.32	0.1887
YOLOv10	92.18	0.1609
YOLOv11	94.46	0.1435
TAS-YOLOv11	95.16	0.1252

TABLE VI. IDENTIFICATION RESULTS OF INSULATOR DEFECTS USING DIFFERENT MODELS

Models	Class	Accuracy	Recall
	Defect-Free	0.8745	0.8617
RTDETR	Defect Type 1	0.8659	0.8569
KIDEIK	Defect Type 2	0.8943	0.8722
	Defect Type 3	0.8741	0.8632
	Defect-Free	0.8918	0.8774
R-CNN	Defect Type 1	0.8901	0.8749
K-CININ	Defect Type 2	0.8792	0.8564
	Defect Type 3	0.8577	0.8513
	Defect-Free	0.9674	0.9519
YOLOv8	Defect Type 1	0.9357	0.9349
YOLOV8	Defect Type 2	0.9290	0.9125
	Defect Type 3	0.9293	0.9123
	Defect-Free	0.9666	0.9667
YOLOv10	Defect Type 1	0.9381	0.9305
YOLOVIO	Defect Type 2	0.9374	0.9181
	Defect Type 3	0.9341	0.9183
	Defect-Free	0.9683	0.9557
VOI 0-11	Defect Type 1	0.9375	0.9277
YOLOv11	Defect Type 2	0.9434	0.9320
	Defect Type 3	0.9326	0.9379
	Defect-Free	0.9793	0.9632
TAS-YOLOv11	Defect Type 1	0.9653	0.9564
TAS-TOLOVII	Defect Type 2	0.9699	0.9417
	Defect Type 3	0.9603	0.9581

The defect free insulator detection accuracy and recall of TAS-YOLOv11 model are 97.93% and 96.32%, respectively. Compared to the accuracy of the YOLOv11 model, the TAS-YOLOv11 model shows an improvement of over 1 percentage point. In the detection of the most difficult surface defect (defect type 1), the accuracy of the TAS-YOLOv11 model is 96.53%, which is 2.72 percentage points higher than the suboptimal model YOLOv10. The recall rate of traditional R-

CNN models in missing defects (defect type 3) is only 85.13%, which poses a high risk of inaccurate recognition.

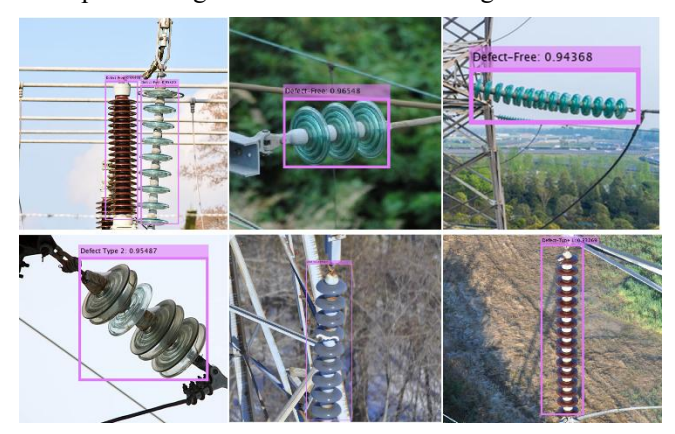


Fig. 8. The results of insulator defect detection based on TAS-YOLOv11 model.

V. CONCLUSION

This study proposes a dual-layer detection model for distribution networks, integrating UAV path planning and insulator defect recognition. In the path planning layer, a power grid inspection UAV path planning model aims to minimize flight distance and maximize image coverage. In addition, a hybrid PSO-MPA algorithm is designed to solve the path planning model of UAV for power grid inspection. The experimental results demonstrate that with a flight step size of one meter, the PSO-MPA algorithm reduces the objective function value by an average of 49.62% compared to the other five algorithms, significantly shortening the path length and improving the integrity of image acquisition for transmission facilities. In the insulator defect recognition layer, a TSA-YOLOv11 model was developed, which introduces a task decoupling allocation module (TSA) to separate positioning and classification tasks, aiming to solve the feature conflict problem of traditional models. The average accuracy of insulator defect detection reached 96.87%, and the recall rate of high-risk damaged defects increased to 94.17%. In future research, combining reinforcement learning with proposed models to construct an online inspection system will be a key focus.

ACKNOWLEDGMENT

This work was supported by the Science and Technology Project of China Southern Power Grid Co., Ltd. under Grants YNKJXM20240219 and YNKJXM20240472.

REFERENCES

- [1] H. Liu et al., "Study on UAV Parallel Planning System for Distribution networks Project Acceptance Under the Background of Industry 5.0," IEEE Transactions on Industrial Informatics, vol. 18, no. 8, pp. 5537-5546, Aug. 2022, doi: 10.1109/TII.2022.3142723.
- [2] P. Hamelin et al., "Discrete-time control of LineDrone: An assisted tracking and landing UAV for live power line inspection and maintenance," 2019 International Conference on Unmanned Aircraft Systems (ICUAS), Atlanta, GA, USA, 2019, pp. 292-298, doi: 10.1109/ICUAS.2019.8798137.
- [3] N. Jain, J. Bedi, A. Anand and S. Godam, "A Transfer Learning Architecture to Detect Faulty Insulators in Powerlines," IEEE

- Transactions on Power Delivery, vol. 39, no. 2, pp. 1002-1011, April 2024, doi: 10.1109/TPWRD.2024.3353203.
- [4] Haizhou Zhang and Shengnan Xu, "Path Planning Technology for Unmanned Aerial Vehicle Swarm Based on Improved Jump Point Algorithm" International Journal of Advanced Computer Science and Applications (IJACSA), 16 (4), 2025. http://dx.doi.org/10.14569/IJACSA.2025.0160426
- [5] Wang Tingyu, Sun Xia, Liu Jiaxing and Zhang Yue, "A Deep Learning Based Detection Method for Insulator Defects in High Voltage Distribution networks" International Journal of Advanced Computer Science and Applications (IJACSA), 15 (10), 2024. http://dx.doi.org/10.14569/IJACSA.2024.0151040
- [6] M. He, L. Qin, X. Deng and K. Liu, "MFI-YOLO: Multi-Fault Insulator Detection Based on an Improved YOLOv8," IEEE Transactions on Power Delivery, vol. 39, no. 1, pp. 168-179, Feb. 2024, doi: 10.1109/TPWRD.2023.3328178.
- [7] H. Liu, Y. P. Tsang, C. K. M. Lee and C. H. Wu, "UAV Trajectory Planning via Viewpo int Resampling for Autonomous Remote Inspection of Industrial Facilities," IEEE Transactions on Industrial Informatics, vol. 20, no. 5, pp. 7492-7501, May 2024, doi: 10.1109/TII.2024.3361019.
- [8] A. Sonny, S. R. Yeduri and L. R. Cenkeramaddi, "Autonomous UAV Path Planning Using Modified PSO for UAV-Assisted Wireless Networks," IEEE Access, vol. 11, pp. 70353-70367, 2023, doi: 10.1109/ACCESS.2023.3293203.
- [9] J. Rückin, F. Magistri, C. Stachniss and M. Popović, "An Informative Path Planning Framework for Active Learning in UAV-Based Semantic Mapping," IEEE Transactions on Robotics, vol. 39, no. 6, pp. 4279-4296, Dec. 2023, doi: 10.1109/TRO.2023.3313811.
- [10] D. Scott, S. G. Manyam, I. E. Weintraub, D. W. Casbeer and M. Kumar, "Noise Aware Path Planning and Power Management of Hybrid Fuel UAVs," IEEE Transactions on Automation Science and Engineering, vol. 22, pp. 8227-8238, 2025, doi: 10.1109/TASE.2024.3481998.
- [11] J. V. Shirabayashi and L. B. Ruiz, "Toward UAV Path Planning Problem Optimization Considering the Internet of Drones," IEEE Access, vol. 11, pp. 136825-136854, 2023, doi: 10.1109/ACCESS.2023.3339227.
- [12] Xiuzhu Zhang, "Path Planning and Control of Intelligent Delivery UAV Based on Internet of Things and Edge Computing" International Journal of Advanced Computer Science and Applications (IJACSA), 15 (3), 2024. http://dx.doi.org/10.14569/IJACSA.2024.01503107
- [13] E. Yanmaz, H. M. Balanji and İ. Güven, "Dynamic Multi-UAV Path Planning for Multi-Target Search and Connectivity," IEEE Transactions on Vehicular Technology, vol. 73, no. 7, pp. 10516-10528, July 2024, doi: 10.1109/TVT.2024.3363840.
- [14] J. Li, Y. Zhu, C. Li and Z. Song, "A Motion Camouflage-Inspired Path Planning Method for UAVs Based on Reinforcement Learning," IEEE Transactions on Aerospace and Electronic Systems, vol. 61, no. 2, pp. 4105-4114, April 2025, doi: 10.1109/TAES.2024.3496417.
- [15] Binbin Tu, Fei Wang, Xiaowei Han and Xibei Fu, "Q-learning Guided Grey Wolf Optimizer for UAV 3D Path Planning" International Journal of Advanced Computer Science and Applications (IJACSA), 15 (7), 2024. http://dx.doi.org/10.14569/IJACSA.2024.0150747
- [16] Haishi Liu, Yuxuan Sun, Nan Pan, Qiyong Chen, Xiaojue Guo, Dilin Pan, "Multi-UAV Cooperative Task Planning for Border Patrol based on Hierarchical Optimization" in Journal of Imaging Science and Technology, vol.65, pp 040402-1 040402-8, 2021, doi: https://doi.org/10.2352/J.ImagingSci.Technol.2021.65.4.040402
- [17] J. Chen, Z. Hu, W. Wu, Y. Zhao and B. Huang, "LKPF-YOLO: A Small Target Ship Detection Method for Marine Wide-Area Remote Sensing Images," IEEE Transactions on Aerospace and Electronic Systems, vol. 61, no. 2, pp. 2769-2783, April 2025, doi: 10.1109/TAES.2024.3476459.
- [18] Y. Li, D. Feng, Q. Zhang and S. Li, "HRD-YOLOX Based Insulator Identification and Defect Detection Method for Distribution networks," IEEE Access, vol. 12, pp. 22649-22661, 2024, doi: 10.1109/ACCESS.2024.3363430.
- [19] X. Zhang, B. Cui, Z. Wang and W. Zeng, "Loader Bucket Working Angle Identification Method Based on YOLOv5s and EMA Attention

- Mechanism," IEEE Access, vol. 12, pp. 105488-105496, 2024, doi: 10.1109/ACCESS.2024.3435146.
- [20] Z. Zhao, H. Wang, H. Li, J. Yang and P. Yu, "A Pixel Expansion-Based Improvement in Dense Nesting Structures for Infrared Small Target Detection," IEEE Geoscience and Remote Sensing Letters, vol. 22, pp. 1-5, 2025, Art no. 6005205, doi: 10.1109/LGRS.2025.3547899.
- [21] Y. Li, Y. Lu, K. Wu, Y. Fang, C. Zheng and J. Zhang, "Intelligent Inspection System for Power Insulators Based on AAV on Complex Weather Conditions," IEEE Transactions on Applied Superconductivity, vol. 34, no. 8, pp. 1-4, Nov. 2024, Art no. 9003204, doi: 10.1109/TASC.2024.3465368.
- [22] Z. Xuan, J. Ding and J. Mao, "Intelligent Identification Method of Insulator Defects Based on CenterMask," IEEE Access, vol. 10, pp. 59772-59781, 2022, doi: 10.1109/ACCESS.2022.3179975.
- [23] Z. Wang, Y. Zhu, Z. Ji, S. Liu and Y. Zhang, "An Efficient YOLOv8-Based Model With Cross-Level Path Aggregation Enabling Personal Protective Equipment Detection," IEEE Transactions on Industrial Informatics, vol. 20, no. 11, pp. 13003-13014, Nov. 2024, doi: 10.1109/TII.2024.3431045.
- [24] A. Faramarzi, M. Heidarinejad, S. Mirjalili, and A. H. Gandomi, "Marine Predators Algorithm: A nature-inspired metaheuristic," Expert Systems With Applications, vol. 152, Art. no. 113377, 2020, doi: 10.1016/j.eswa.2020.113377

- [25] H. Su et al., "RIME: A physics-based optimization," Neurocomputing, vol. 532, pp. 183–214, 2023, doi: 10.1016/j.neucom.2023.02.010
- [26] A. A. Heidari, S. Mirjalili, H. Faris, I. Aljarah, M. Mafarja, and H. Chen, "Harris hawks optimization: Algorithm and applications," Future Generation Computer Systems, vol. 97, pp. 849–872, 2019, doi: 10.1016/j.future.2019.02.028
- [27] A.-Q. Tian, F.-F. Liu, and H.-X. Lv, "Snow Geese Algorithm: A novel migration-inspired meta-heuristic algorithm for constrained engineering optimization problems," Applied Mathematical Modelling, vol. 126, pp. 327–347, 2024, doi: 10.1016/j.apm.2023.10.045
- [28] Sun, H., Wang, Y., Du, J., & Wang, R. (2025). MFE-YOLO: A Multi-feature Fusion Algorithm for Airport Bird Detection. ICCK Transactions on Intelligent Systematics, 2(2), 85–94. https://doi.org/10.62762/TIS.2025.323887
- [29] Hamza, M., Ali, I., Ali, S., Khan, W., Shah, S.M., & Haq, I.U. (2025). Leveraging Machine Learning and Deep Learning for Advanced Malaria Detection Through Blood Cell Images. ICCK Journal of Image Analysis and Processing, 1(1), 17–26. https://doi.org/10.62762/JIAP.2025.514726
- [30] Akhtar, F., & Mahum, R. (2025). IRV2-hardswish Framework: A Deep Learning Approach for Deepfakes Detection and Classification. ICCK Journal of Image Analysis and Processing, 1(1), 45–56. https://doi.org/10.62762/JIAP.2025.421251